Catalysis Today 160 (2011) 70–78

Catalysis Today

journal homepage: www.elsevier.com/locate/cattod

Adsorption and decomposition of ethanol on supported Au catalysts☆

A. Gazsi[b], A. Koós[a], T. Bánsági[b], F. Solymosi[a,b,*]

[a] Reaction Kinetics Research Group, Chemical Research Centre of the Hungarian, Academy of Sciences, P.O. Box 168, H-6701 Szeged, Hungary
[b] Department of Physical Chemistry and Materials Science, University of Szeged, P.O. Box 168, H-6701 Szeged, Hungary

ARTICLE INFO

Article history:
Available online 9 June 2010

Keywords:
FTIR spectroscopy
Decomposition of ethanol
Hydrogen production
Reaction of acetaldehyde
Au catalyst
CeO_2 support

ABSTRACT

The adsorption and reactions of ethanol are investigated on Au nanoparticles supported by various oxides and carbon Norit. The catalysts are characterized by means of XPS. Infrared spectroscopic studies reveal the dissociation of ethanol to ethoxy species at 300 K on all the oxidic supports. The role of Au is manifested in the enhanced formation of ethoxy species on Au/SiO_2, and in increased amounts of desorbed products in the TPD spectra. The supported Au particles mainly catalyse the dehydrogenation of ethanol, to produce hydrogen and acetaldehyde. An exception is Au/Al_2O_3, where the main process is dehydration to yield ethylene and dimethyl ether. C–C bond cleavage occurs to only a limited extent on all samples. As regards to the production of hydrogen, the most effective catalyst is Au/CeO_2, followed by Au/SiO_2, Au/Norit, Au/TiO_2 and Au/MgO. A fraction of acetaldehyde formed in the primary process on Au/CeO_2 is converted above 623 K into 2-pentanone and 3-penten-2-one. The decomposition of ethanol on Au/CeO_2 follows first-order kinetics. The activation energy of this process is 57.0 kJ/mol. No deactivation of Au/CeO_2 is observed during ~10 h at 623 K. It is assumed that the interface between Au and partially reduced CeO_2 is responsible for the high activity of the Au/CeO_2 catalyst.

1. Introduction

The demand for pure hydrogen for electric vehicles and power stations has initiated tremendous interest in the production of hydrogen [1–3]. Water, methane, methanol and ethanol are potential primary sources of hydrogen, and there is clearly a need for an effective, stable and cheap catalyst for the generation of relatively pure hydrogen from these compounds, all of which have advantages and disadvantages. In principle, its high H/C ratio would seem to suggest methane as the best material for the production of hydrogen [4,5]. Supported Pt metals effectively catalyse the decomposition of methane, but the deposition of carbon on the catalysts leads to early deactivation [6–12]. The H/C ratio is similarly high in methanol, but its synthesis requires hydrogen, and its toxic nature must also be borne in mind. Ethanol has the advantage that it can be manufactured by the fermentation of crops and biomass-derived compounds, and its storage and transportation are comparatively easy. The C–C bond cleavage, however, demands an active catalyst. Moreover, the deactivation of Pt metals by acetate is a significant drawback [13–15].

In an effort to replace the expensive noble metals, the catalyst Mo_2C prepared on multiwall carbon nanotube or carbon Norit was found to be effective and stable in the decomposition and reforming of ethanol [16,17], methanol [18] and dimethyl ether [19]. The pioneering work by Haruta [20] and Hutchings [21] indicated that supported Au exhibited unusually high activity in the oxidation of carbon monoxide and in several other reactions, and it was expected that Au nanoparticles may exhibit similar catalytic activity in the reaction of alcohol, when oxidation of both carbon atoms and hydrogen is necessary. Whereas a number of studies have been devoted to the decomposition of methanol on supported Au [22–28], only a few papers deal with the reactions of ethanol on this catalyst. Idriss et al. [29] studied the oxidation of ethanol on Au/CeO_2, and Guan and Hensen [30] recently examined the dehydrogenation of ethanol on Au nanoparticles deposited on various SiO_2 supports. A strong influence of the Au particle size was observed. It was noteworthy that, in the presence of oxygen, the intrinsic activity of Au/SiO_2 increased considerably.

In the present work we give an account of the decomposition and reforming of ethanol on supported Au catalysts, with particular emphasis on the effects of the supports.

2. Experimental

2.1. Materials and preparation of the catalysts

The following compounds were used as supports. CeO_2 (ALFA AESAR, 50 m^2/g), Al_2O_3 (Degussa P110 C1, 100 m^2/g), MgO (DAB 6,

☆ This paper is for a special issue entitled "Heterogeneous Catalysis by Metals: New Synthetic Methods and Characterization Techniques for High Reactivity" guest edited by Jinlong Gong and Robert Rioux.

* Corresponding author at: Department of Physical Chemistry and Materials Science, University of Szeged, P.O. Box 168, H-6701 Szeged, Hungary.
Fax: +36 62 420 678.
E-mail address: fsolym@chem.u-szeged.hu (F. Solymosi).

0920-5861/$ – see front matter © 2010 Elsevier B.V. All rights reserved.
doi:10.1016/j.cattod.2010.05.007

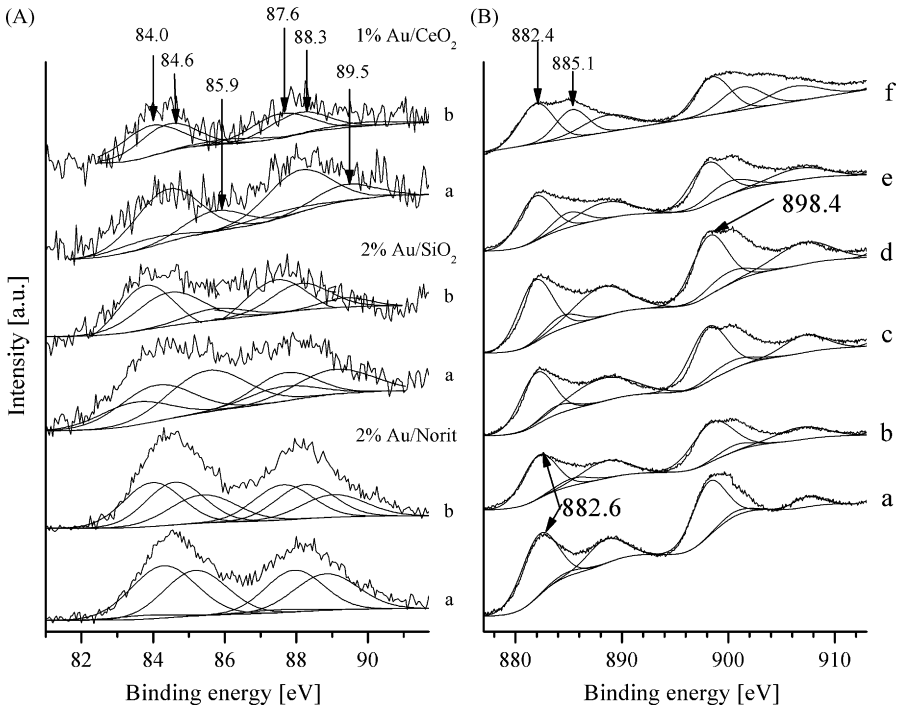

Fig. 1. (A) XPS spectra in the Au 4f region of 1% Au/CeO_2, 2% Au/SiO_2 and 2% Au/Norit: (a) oxidized at 573 K, (b) reduced at 673 K for 1 h. (B) XPS spectra of 1% Au/CeO_2 for cerium region: (a) oxidized at 573 K, then reduced at different temperatures, (b) 373 K, (c) 473 K, (d) 573 K, (e) 673 K and (f) 773 K.

170 m^2/g), TiO_2 (Degussa P25, 50 m^2/g), SiO_2 (CAB-O-SiL, 198 m^2/g) and activated carbon Norit (ALFA AESAR, 859 m^2/g). Carbon Norit was purified by treatment with HCl (10%) for 12 h at room temperature. Supported Au catalysts with an Au loading of 1, 2 or 5 wt% were prepared by a deposition–precipitation method. $HAuCl_4$·aq (p.a., 49% Au, Fluka AG) was first dissolved in triply distilled water. After the pH of the aqueous $HAuCl_4$ solution had been adjusted to 7.5 by the addition of 1 M NaOH solution, a suspension was prepared with the finely powdered oxidic support, and the system was kept at 343 K for 1 h under continuous stirring. The suspension was then aged for 24 h at room temperature, washed repeatedly with distilled water, dried at 353 K and calcined in air at 573 K for 4 h. The fragments of catalyst pellets were oxidized at 673 K and reduced at 673 K for 1 h in situ. The sizes of the Au nanoparticles were determined with an electron microscope: 2–3 nm for 1% Au/CeO_2, 3–4 nm for 1% Au/SiO_2, 6–7 nm for 1% Au/TiO_2, 6–7 nm for 1% Au/MgO, 5–6 nm for 1% Au/Norit.

2.2. Methods

Catalytic reactions were carried out at 1 atm in a quartz tube (8 mm id) that served as a fixed-bed, continuous flow reactor. The flow rate was in general 60 ml/min. The carrier gas was Ar, which was bubbled through ethanol at room temperature: the ethanol content was ~9.0–10%. In general, 0.3 g of loosely compressed catalyst sample was used. After reduction of the catalyst, the reactor was flushed with Ar for 15 min, and the sample was cooled in an Ar flow to the lowest reaction temperature investigated. After the Ar had been replaced by the reacting gas mixture, the reactor was gradually heated to selected temperatures, at which the gases were analysed with an HP 5890 gas chromatograph fitted with PORAPAK Q and PORAPAK S packed columns, or in certain cases with an Agilent 6890N gas chromatograph (column: HP Plot-Q) combined with an Agilent MSD 5795 mass spectrometer. In the study of the reactions of ethanol–water mixtures of different compositions, the reactants were introduced into an evaporator with the aid of an infusion pump (MEDICOR ASSISTOR PCI flow rate: 1.0 ml liquid/h): the evaporator was flushed with an Ar flow (36 ml/min). The alcohol- or alcohol–water-containing Ar flow entered the reactor through an externally heated tube in order to avoid condensation. The conversion of ethanol was calculated by taking into account the amount consumed. To establish the efficiency of the catalyst with regard to the production of hydrogen, the percentage of hydrogen formed with respect to the hydrogen content of the ethanol decomposed was determined. This value is termed H_2 eff.

DRIFTS analyses were performed in a diffuse reflectance infrared cell (Spectra Tech) with a CaF_2 window, on a BioRad FTS-155 spectrometer with a wavenumber accuracy of $\pm 4\,cm^{-1}$. The same instrument was used for FTIR spectroscopic measurements. Two types of experiments were carried out. Either the reduced catalyst was exposed to ethanol at room temperature for 30 min, and the sample was then heated up during continuous degassing to higher temperatures, where the spectra were taken, or the IR spectra were registered in situ during the high-temperature reaction. The spectrum of the sample after the reduction step was used as background. Thermal desorption measurements (TPD) were carried out in the catalytic reactor. The catalysts were treated with ethanol/Ar containing 10% ethanol at ~300 K for 30 min, and then flushed with Ar for 30 min. The TPD was carried out in an Ar flow (20 ml/min) with a ramp at 5 K/min from 300 K to ~950 K. Desorbing products were analysed by gas chromatography. Transmission electron microscopy (TEM) images were taken with a Philips CM 20 and a Morgagni 268 D electron microscope at 300 K. Approximately 1 mg of catalyst was placed on a TEM grid. X-ray photoelectron spectroscopy (XPS) images were taken with a Kratos XSAM 800 instrument, using non-monochromatic Al Kα radiation ($h\nu = 1486.6$ eV) and a 180° hemispherical analyser at a base pressure of 1×10^{-9} mbar. Binding energies were referenced to the C 1s binding energy (BE) (285.1 eV), with the exception of Au/SiO_2, where the Si 2p core level at 103.4 eV was used as reference.

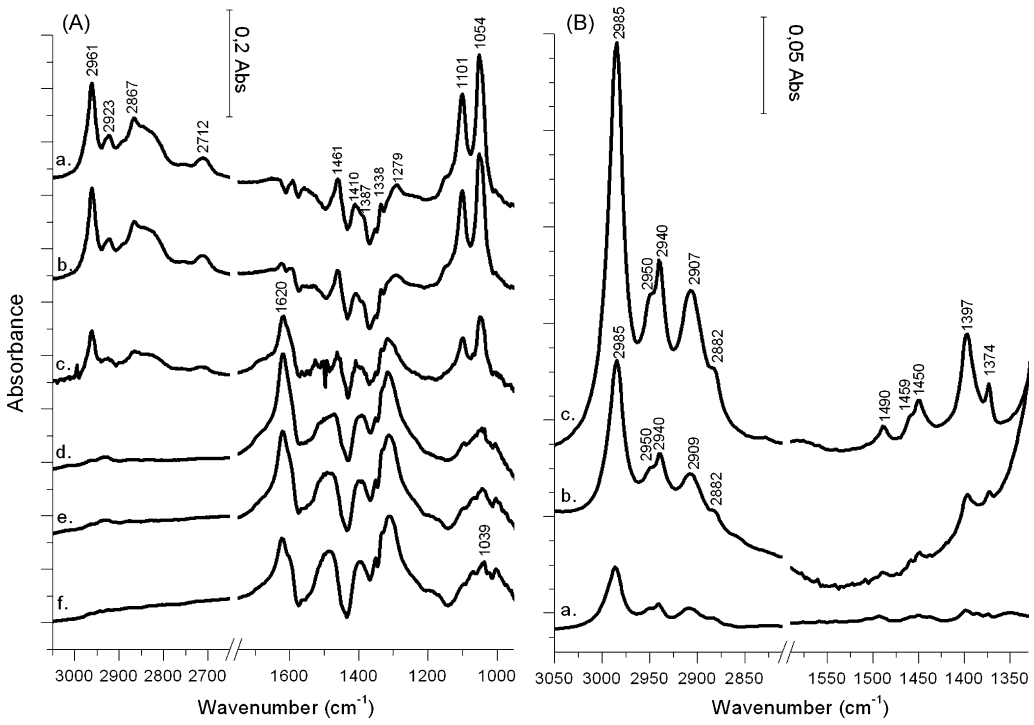

Fig. 2. (A) FTIR spectra following the adsorption of ethanol on 1% Au/CeO_2 at 300 K and after subsequent degassing at different temperatures: (a) 300 K, (b) 373 K, (c) 473 K, (d) 573 K, (e) 673 K, (f) 773 K. (B) FTIR spectra of SiO_2 (a); 1% Au/SiO_2 (b) and 5% Au/SiO_2 (c) after heating the adsorbed ethanol at 300–473 K under continuous evacuation.

3. Results

3.1. XPS characterization of Au samples

The XPS spectra of some supported Au catalysts are presented in Fig. 1. For quantitative evaluation of the Au 4f region, we accepted the BEs of three Au states: 84.0 eV for Au^0, 84.6 eV for Au^{1+} and 85.9 eV for Au^{3+} [29,31,32]. We used 3.65 eV for Au $4f_{5/2}$ spin–orbit splitting, with ~2.0 eV FWHM for the fitted peaks. Accordingly, the XP spectrum for the oxidized 1% Au/CeO_2 sample in the Au $4f_{7/2}$ region showed that most of the Au was in the Au^+ and Au^{3+} states. After reduction of the sample at 673 K, the BE for Au^{3+} almost disappeared that of Au^0 developed. As concerns the XPS region of CeO_2 in the oxidized Au/CeO_2 catalyst, the dominant peaks at 882.6 and 898.4 eV were due to Ce^{4+}. The shoulders at 885.1 and 900.4 eV, however, revealed the presence of Ce^{3+} in the starting material [33–35]. These features became more evident after the reduction of the Au/CeO_2 at higher temperatures. After the oxidation of the 2% Au/SiO_2, the peaks in the Au 4f region demonstrated the presence of Au^{3+}, Au^+ and Au^0. The reduction at 673 K increased the intensity of the peak for Au^0, but, similarly as for 1% Au/CeO_2, did not eliminate Au^+ on the surface. On the oxidized Au/Norit sample, there were equal amounts of Au^{3+} and Au^+. After reduction, the BE peak for Au^0 also appeared, but signals for Au^{3+} and Au^+ were still present.

3.2. Infrared spectroscopic measurements

Fig. 2A depicts the IR spectra of ethanol adsorbed on 1% Au/CeO_2 (T_R = 673 K) at 300 K and heated to different temperatures under continuous degassing. At 300 K, intense absorption bands were observed at 2961, 2923, 2867 and 2712 cm^{-1} in the C–H stretching region. In the low-frequency range, absorption bands were identified at 1461, 1410, 1387, 1338, 1279, 1101 and 1054 cm^{-1}. Heating the sample caused the attenuation of all the bands. A new spectral feature appeared at 1620 cm^{-1}, the intensity of which increased up to 573 K, and then decreased. Virtually identical spectra were measured following the adsorption of ethanol on the CeO_2, with the difference that the band at 1620 cm^{-1} was missing. Similar spectral features were found for Au/Al_2O_3 and Au/MgO. The results obtained for Au/SiO_2 deserve special mention. The advantage of this sample is that ethanol adsorbs only weakly on silica and the formation of ethoxy species is very limited [36], and it may therefore be expected that the vibration bands observed are due to the species attached to Au particles. In order to eliminate the absorption bands arising from weakly adsorbed ethanol, the adsorbed layer was heated to 473 K under continuous degassing. The TPD experiments (see next section) indicated that this treatment is sufficient for the desorption of ethanol. The IR spectrum for pure SiO_2 revealed only very weak bands, but the deposition of 1% Au caused significant increases in the intensities of the bands at 2985, 2950, 2940, 2907, 2882, 1490, 1459, 1450, 1397 and 1374 cm^{-1}. These vibrations were very strong on 5% Au/SiO_2, though their positions remained practically unchanged. The band at 1620 cm^{-1} did not develop. IR spectra are displayed in Fig. 2B. It is noteworthy that the adsorption of ethanol on all the samples except Au/SiO_2 caused the well-known negative feature in the OH frequency range between 3600 and 3700 cm^{-1}, indicating that surface OH groups were consumed in the reaction with ethanol to give the ethoxy radical:

$$C_2H_5OH_{(a)} + OH_{(a)} = C_2H_5O_{(a)} + H_2O_{(g)} \quad (1)$$

Table 1 lists the characteristic vibrations of the ethoxy species on the different solids, and their possible assignments.

3.3. Thermal desorption measurements

TPD spectra for the various products after the adsorption of ethanol on the Au catalysts at ~300 K are presented in Fig. 3. For pure CeO_2 the release of adsorbed ethanol started slightly above 300 K and peaked at ~370–400 K. At 580 K, the desorption of a small amount of hydrogen was detected. In contrast, the desorption of several compounds was registered from the 1%

Table 1
IR vibrational frequencies and their assignment for ethoxy species produced following the adsorption of ethanol on cerium-based catalysts at 300 K.

Vibrational mode	CeO_2 [38]	CeO_2 [present work]	Rh/CeO_2 [37]	Pt/CeO_2 [14]	Au/CeO_2 [29]	Au/CeO_2 [present work]	Au/SiO_2 [present work]
$\nu_{as}(CH_3)$	2960	2966	2981	2981	2971	2961	2985
$\nu_{as}(CH_2)$	–	2927	2934	–	2933	2923	2940
$\nu_s(CH_3)$	2836	2896	2911	2896	2904	–	2907
$\nu_s(CH_2)$	–		2878	2872	2875	2867	2882
$\delta_{as}(CH_2)$	1473	1447	1478	–	1478	–	1490
$\delta_{as}(CH_3)$	–		1450	1445	1449	1461	1450
$\delta_s(CH_3)$	1383		1399	1391	1399	1387	1397
$\delta_s(CH_2)$	–	1297	–	1264	1362		1374
$\omega(CH_2)$	–		–	–	1333		
ν(OC) mono-	1107	1114	1080	1100	1109	1101	
ν(OC)/ν(CC)	–	1064	–	1072	1065	1084	
ν(OC) bi-	1057	1048	1038	1042	1038		

Au/CeO_2 sample (Fig. 3A). The quantity of ethanol ($T_p \sim 340$ K) desorbed from 1% Au/CeO_2 was practically the same as measured for pure CeO_2. However, greater amounts of hydrogen with different peak temperatures (T_p = 425, 600 and 695 K) were registered. Acetaldehyde ($T_p \sim 530$ K), carbon monoxide ($T_p \sim 540$, 615 and 675 K) and a small amount of methane were also evolved. When the Au content was increased to 5%, larger quantities of the same compounds desorbed, but with almost identical T_p values. Several compounds desorbed from Au/SiO_2: ethanol ($T_p \sim 350$ K), acetaldehyde (T_p = 460 K), hydrogen (T_p = 460 and 675 K), methane (T_p = 650 K) and ethylene (T_p = 680 K) (Fig. 3B). Control measurements revealed that pure silica adsorbs ethanol only weakly, which is released with T_p = 350 K.

3.4. Decomposition of ethanol

Fig. 4A illustrates the conversion of ethanol on Au supported by various materials. The catalytic performance of the Au catalyst was dramatically influenced by the nature of the support. On the most active catalysts, Au/Al_2O_3 and Au/CeO_2, the decomposition began above ~475 K and total conversion was reached at 773 K. On the less active Au/MgO, the extent of decomposition was only ~37% even at 773 K. The conversion measured in the temperature range 573–673 K demonstrated that the efficiency of the supports decreased in the sequence $Al_2O_3 > CeO_2 > TiO_2 >$ Norit $> SiO_2 >$ MgO. Fig. 4B presents the rates of formation of hydrogen, and Fig. 4C presents the effective yields of hydrogen on the different samples.

There were also marked differences between the catalysts from the aspect of the product distribution, as illustrated for the various carbon-containing products on some selected catalysts in Fig. 5. On the most active catalyst, Au/Al_2O_3, the dehydrating property of alumina led to the production of diethyl ether, ethylene and water. The formation of hydrogen was hardly detectable. In contrast, following the deposition of Au on carbon Norit, which can be considered a completely inactive material towards the decomposition of ethanol, the major products were hydrogen and acetaldehyde. Small amounts of carbon monoxide and methane were also identified, mainly above 623 K (Fig. 5A). On Au/SiO_2, hydrogen, acetaldehyde, diethyl ether and ethylene were produced at 573–623 K. At higher temperatures the amount of acetaldehyde decreased, and those of ethylene and acetone increased (Fig. 5B).

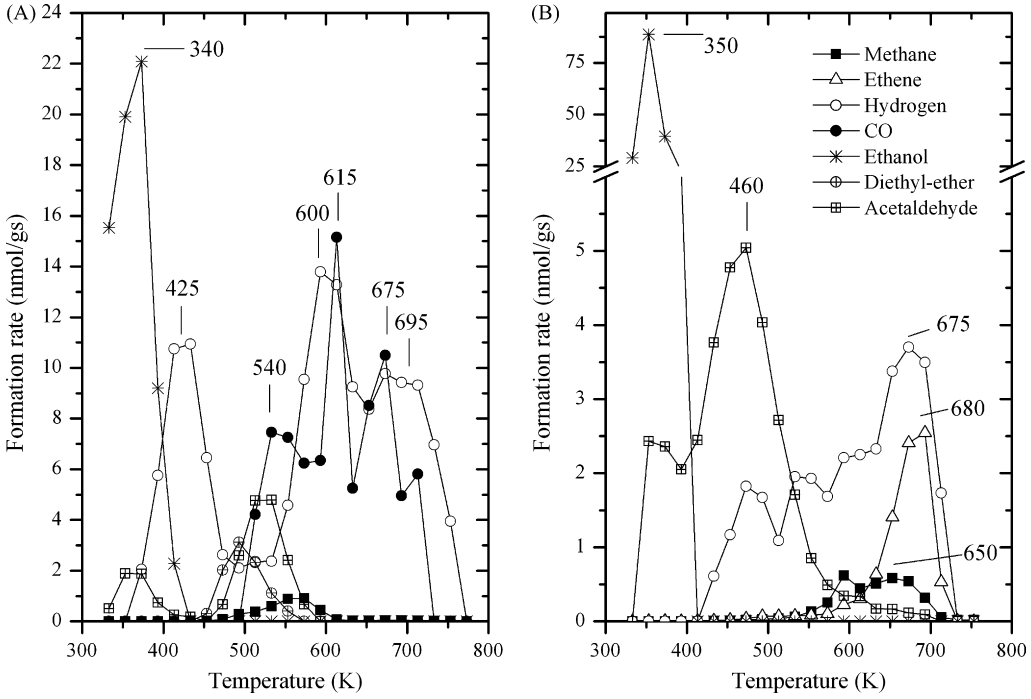

Fig. 3. TPD spectra following the adsorption of ethanol on 1% Au/CeO_2 (A), and 2% Au/SiO_2 (B) at 300 K.

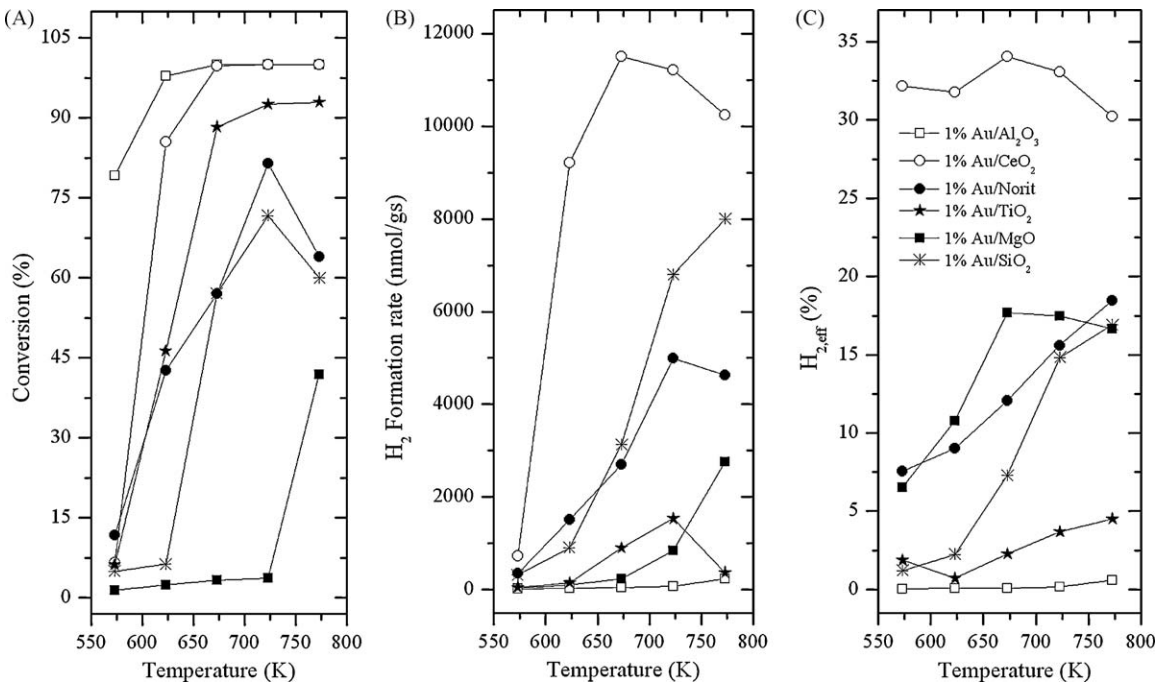

Fig. 4. Conversion of ethanol (A), rate of hydrogen formation (B) and the effective yield of H_2 production (C) on Au deposited on various supports as a function of temperature.

On the less effective Au/MgO, where the decomposition was very limited below 673 K, hydrogen and acetaldehyde were produced.

A very complex picture emerged for the CeO_2-based samples. Pure CeO_2 alone exhibited catalytic activity towards the decomposition of ethanol above 600 K, yielding H_2, C_2H_4, CO_2, CH_4, CO and CH_3CHO, in quantities decreasing in this sequence. The deposition of Au on CeO_2 markedly influenced the product distribution. Whereas hydrogen and acetaldehyde were formed in the same ratio on 1% Au/CeO_2 up to 573 K, above this temperature the ratio was altered markedly: the extent of hydrogen formation increased dramatically, while that of acetaldehyde decreased. New major products were acetone, ethylene, methane, 2-pentanone ($C_5H_{10}O$), 3-penten-2-one (C_5H_8O), carbon monoxide and, in smaller amounts, ethyl acetate, 2-butanone and 2-buten-1-ol. Trace quantities of 1,3-butadiene, toluene, ethyl-butanoate and 2-heptanone were also identified. The evolution of water was observed on all these catalysts, but its amount was not determined.

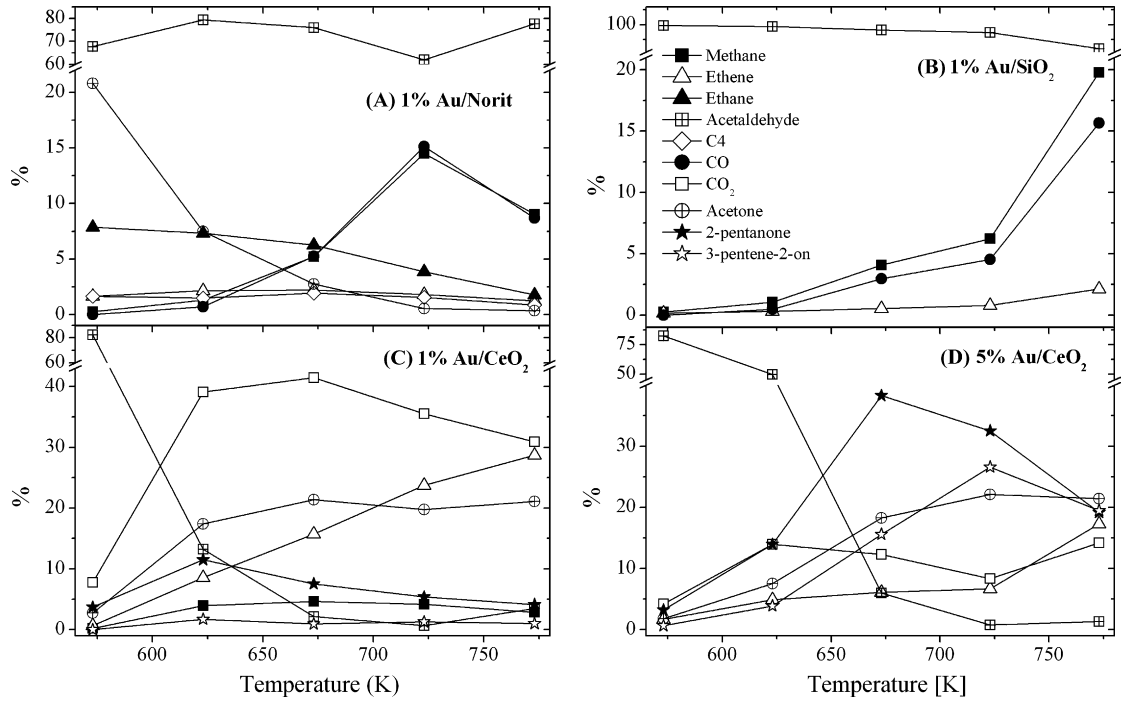

Fig. 5. Distribution of carbon-containing products (in mol.%) formed in the decomposition of ethanol on 1% Au/Norit (A), 1% Au/SiO_2 (B), 1% Au/CeO_2 (C) and 5% Au/CeO_2 (D) at different temperatures.

We devoted some attention to the products 2-pentanone and 3-penten-2-one, which were identified by gas chromatography combined with mass spectrometry. As shown in Fig. 5C and D, their formation started at ~623 K and became more extensive at higher temperatures. The role of the Au content in their production is clearly seen in Fig. 5. It is important to mention that these compounds did not evolve on the other supported Au catalysts. As the absolute and relative amounts of acetaldehyde drastically decreased on Au/CeO_2 samples at and above 623 K without the formation of methane and carbon monoxide, we carried out exploratory experiments on the reactions of acetaldehyde on this catalyst. 2-Pentanone and 3-penten-2-one were formed, together with hydrogen, crotonaldehyde, carbon dioxide, and acetone. Methane and carbon monoxide appeared only at 773 K, in quantities of merely 2–3%.

On the 1% Au/CeO_2 catalyst, we performed kinetic measurements at low conversion. The partial pressure of ethanol was varied, the total flow rate being kept at 60 ml/min by the addition of Ar ballast to the system. The reaction of ethanol under these conditions followed first-order kinetics. Experiments were carried out in the temperature range 523–583 K. The ethanol conversion level ranged between 2.0 and 9.0%. The Arrhenius plots yielded 57.0 kJ/mol for the activation energy of the decomposition of ethanol, and 75.6 kJ/mol for the formation of hydrogen. When the decomposition was followed in time on stream on Au/CeO_2 at 623 K, only a slow decay was experienced in the conversion and product distribution in ~8 h. At 773 K, however, the deactivation was more pronounced.

The addition of water to the ethanol decreased the conversion of the ethanol in the lower-temperature range for the active Au/CeO_2 and Au/Al_2O_3, and total conversion was approached only at 773 K. No appreciable change occurred in the product distribution. Similar features were observed for the other samples.

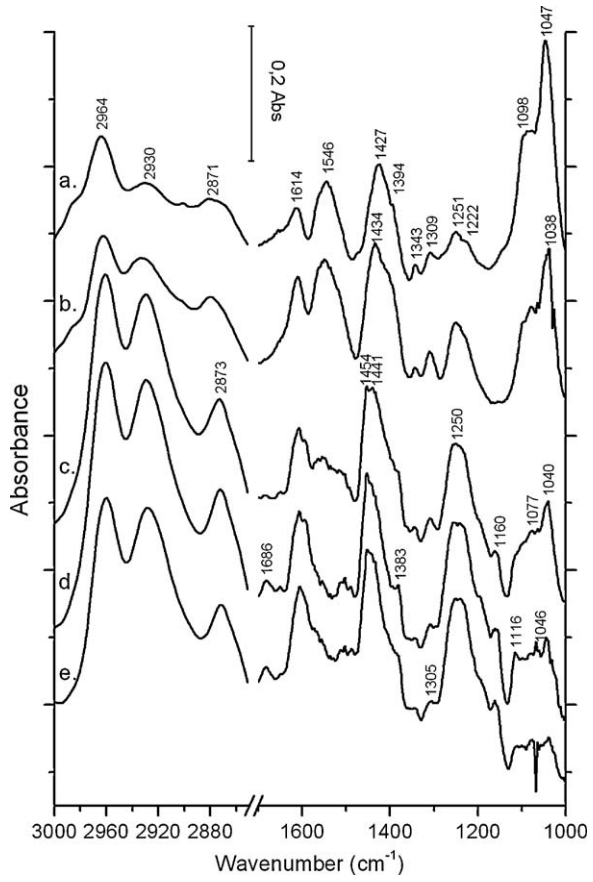

Fig. 6. In situ DRIFT spectra registered on 1% Au/CeO_2 during the decomposition of ethanol at 573–773 K. (a) 573 K, (b) 623 K, (c) 673 K, (d) 723 K, (e) 773 K.

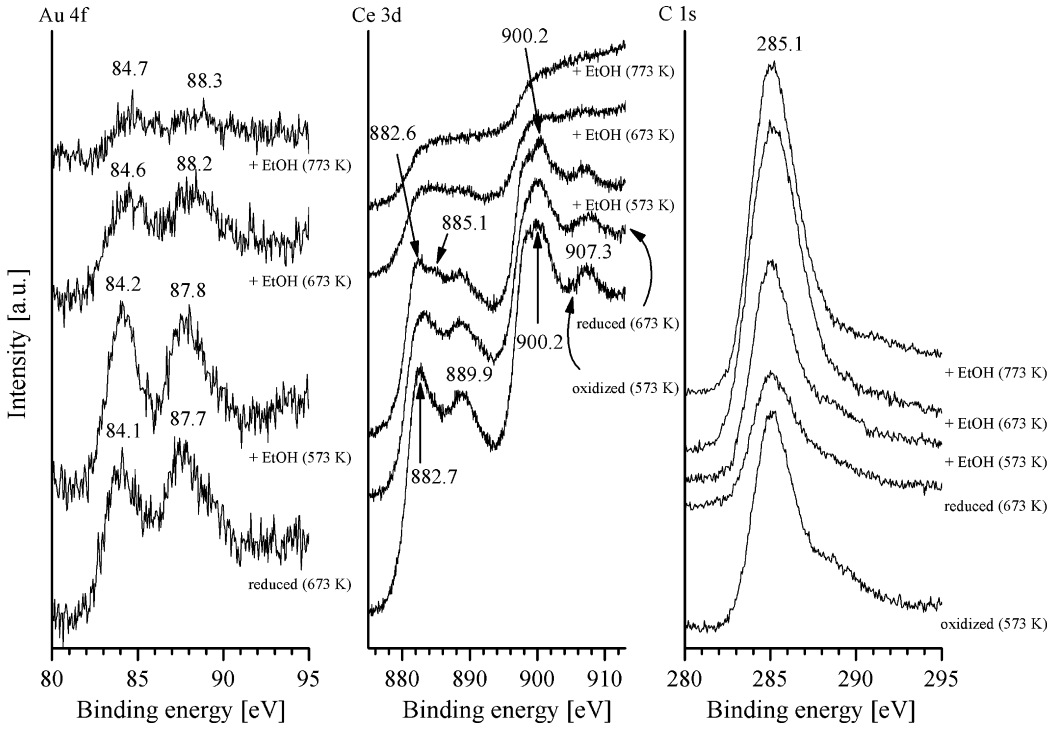

Fig. 7. XPS spectra of 5% Au/CeO_2 taken after the reaction of ethanol at different temperatures.

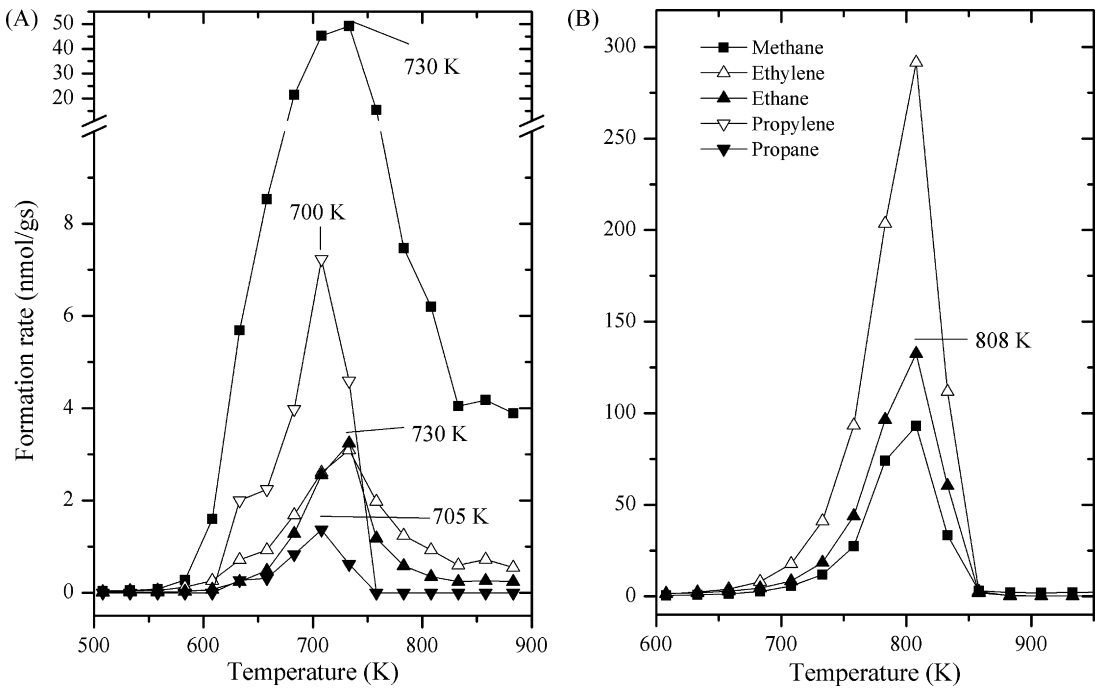

Fig. 8. TPR spectra for 1% Au/CeO_2 (A) and 2% Au/SiO_2 (B) after decomposition of ethanol at 623 K for 13 h.

3.5. *In situ FTIR study*

Fig. 6 displays DRIFT spectra registered during the decomposition of ethanol on 1% Au/CeO_2 at different reaction temperatures. At 573–623 K, well-detectable bands were seen in the C–H stretching region, at 2964, 2930 and 2871 cm^{-1}. In the lower-frequency range, intense bands were observed at 1614, 1546, 1427, 1394, 1251, 1098 and 1047 cm^{-1}. As the reaction temperature was gradually raised to 673–773 K, a new absorption band developed at ~1686 cm^{-1}. At 723 K, the major bands were located at 2961, 2929, 2873, 1686, 1610, 1594, 1454, 1441, 1383, 1250, 1160, 1077 and 1046 cm^{-1}. Vibration bands of carbon dioxide already appeared at 2361 and 2333 cm^{-1} at 573 K, and became stronger above this temperature (not shown).

3.6. *XPS study of the catalysts in the course of the reaction*

In order to obtain deeper insight into the events on the catalyst surface during the reaction, the decomposition of ethanol was followed on supported Au in a minireactor attached to the XPS system. From time to time, the sample was degassed and introduced into the analyser chamber. Relevant XPS spectra are displayed in Fig. 7. When the reaction was performed below 673 K on 5% Au/CeO_2, no or very little alteration was observed in the positions of the BEs of Au and Ce. As the temperature was elevated, the BE of the Au $4f_{7/2}$ moved from 84.1 to 84.6 eV at 673 K and to 84.7 at 773 K, indicating partial oxidation of the Au. The intensities of the BEs of Ce^{3+} at 885.1 and 900.2 eV became more pronounced, suggesting the reduction of Ce^{4+} during the reaction. At the same time at 673–773 K, the O 1s signal decreased and the C 1s signal increased markedly, pointing to a considerable deposition of carbon-containing species on the catalyst, very likely on the CeO_2 support. The BEs for 2% Au/Norit remained practically the same during the catalytic reaction. A new weak O 1s signal appeared at 533.3 eV. The decomposition of ethanol on 2% Au/SiO_2 caused a shift in the position of Au $4f_{7/2}$ by 0.2 eV at 573 K. No further change occurred at higher reaction temperatures. In contrast, the reaction of ethanol at 573 K resulted in an increase in intensity of the C 1s peak at 285.1 eV, which was enhanced with elevation of the temperature.

3.7. *TPR measurements*

After completion of the catalytic experiments, TPR measurements were carried out (Fig. 8). The amount and the reactivity of the surface carbonaceous deposit depended on the reaction temperature. After the decomposition of ethanol on 1% Au/CeO_2 at 623 K for 13 h, the surface carbon reacted with hydrogen only above 600 K, resulting in the formation of methane, ethylene, ethane, propylene and propane with T_p = 705–730 K (Fig. 8A). On 2% Au/SiO_2, larger quantities of methane, ethane and ethylene were found, with T_p = 800 K (Fig. 8B). The reactivity of the surface carbon was much less when the ethanol was previously decomposed on 1% Au/CeO_2 at 773 K for ~13 h. In this case, only methane, ethylene and ethane were evolved above 700 K, without well-defined peaks.

4. Discussion

4.1. *Characterization of the catalyst*

Quantitative evaluation of the XPS spectra for oxidized Au samples showed that besides Au^{3+} a fraction of Au is in the Au^{1+} state. Its formation is probably due to X-ray induced reaction. Reduction of Au catalyst at 673 K led to the transformation of Au^{3+} and Au^{1+} to Au^0, but the complete elimination of Au^{1+} was not achieved. The possible reason is that Au^{1+} in the Au nanoparticles is stabilized by the supports. The fact that the BE values of Ce^{3+} already appeared, when Au was deposited onto CeO_2 suggests a strong interaction between Au and CeO_2 resulting in the partial reduction of Ce^{4+}. Similar phenomenon was experienced following the deposition of some Pt metals on CeO_2 [29,35].

4.2. *Adsorption, desorption and reaction of ethanol*

Whereas the interactions of methanol with metal single-crystal surfaces in UHV have been the subject of extensive research [39],

only a few papers are available on Au surfaces [40–44]. Gong and Mullins [43] reported that, on clean Au(1 1 1), ethanol adsorbs only weakly and desorbs molecularly, but the situation is different on supported Au nanoparticles. As ethanol adsorbs dissociatively on most of the oxidic supports, it is not easy to establish the interaction of ethanol with Au particles alone. The silica and Norit samples provide a possibility, as both supports adsorb ethanol only weakly. Whereas from pure SiO_2 we observed only the desorption of weakly bonded ethanol (T_p = 350 K), from Au/SiO_2 hydrogen, acetaldehyde, ethylene and methane were also released, suggesting the presence of adsorbates bonded strongly to Au particles, which are converted into different surface species identified by IR spectroscopy (Fig. 2). These surface compounds decompose only at higher temperatures yielding various products (Fig. 3). The situation was similar when Au was deposited on carbon Norit. As much larger quantities of the products desorbed from Au/CeO_2 in the interval 500–750 K (Fig. 3), we assume that most of the activated ethanol resides on CeO_2. From pure CeO_2, however, we detected the desorption of lower amounts of these products, which indicates that on Au/CeO_2 a fraction of the ethanol activated on the Au migrates from the Au onto the CeO_2. Alternatively, the adsorption of ethanol proceeds at the Au/CeO_2 interface.

Further insight into the surface processes occurring on the Au samples was provided by FTIR spectroscopic measurements. IR study of the adsorption of ethanol on CeO_2 and CeO_2-based catalysts has been the subject of extensive research [29,36,37,45–47]. Although it is not easy to differentiate between molecularly and dissociatively adsorbed ethanol, in view of the results of previous studies (Table 1) the major bands at 2961 and 2867 cm^{-1} for Au/CeO_2 can certainly be assigned to the asymmetric and symmetric stretches, and the peaks at 1101 and 1054 cm^{-1} to the ν(OC) vibrations of the ethoxy group (Fig. 2A). The presence of molecularly adsorbed ethanol is indicated by the absorption band at 1279 cm^{-1}, due to the δ(OH), and at 1387 cm^{-1}, due to $\nu(\delta CH_3)$ of ethanol. As we obtained practically the same spectrum for CeO_2, we may infer that the identified bands are mainly due to adsorbed ethoxy attached to CeO_2. The absorption bands at ~1550 and 1461 cm^{-1} are tentatively assigned to the ν_a(COO) and ν_s(COO) vibrations of the surface acetate complex. The bands at 1620 and 1594 cm^{-1}, which were identified only on Au/CeO_2 at 473–773 K may be attributed to the ν(C=O) and ν(C=C) of crotonaldehyde, which is formed in the reaction of acetaldehyde:

$$C_2H_5O_{(a)} = CH_3CHO_{(a)} + H_{(a)} \quad (2)$$

$$2CH_3CHO = CH_3CH{=}CHCHO + H_2O \quad (3)$$

It is interesting that the absorption bands at 1690–1698 cm^{-1}, due to ν(C=O) and indicative of adsorbed acetaldehyde, did not appear in the spectra of Au/CeO_2 taken at room temperature (Fig. 2). This means that after its formation it is converted at once into crotonaldehyde (Eq. (3)). These adsorbed compounds are very stable on Au/CeO_2 as their absorption bands could not be eliminated even after degassing at 773 K (Fig. 2).

The role of Au in the adsorption and surface reactions of ethanol is clearly demonstrated by the spectroscopic results for Au/SiO_2 samples (Fig. 2B). The weak adsorption bands observed for pure SiO_2 increased dramatically in the presence of Au. The positions of the vibration peaks differed from those measured for Au/CeO_2, and agreed very well with those determined for Rh/CeO_2 [37] (Table 1), which were ascribed to adsorbed ethoxy species.

We may consider another pathway for the dissociation of ethanol, i.e. the cleavage of the C–O bond and formation of the ethyl radical:

$$C_2H_5OH_{(a)} = C_2H_{5(a)} + OH_{(a)} \quad (4)$$

The characteristic vibrations of this CH fragment determined on Rh(1 1 1) are at 2910–2920, 1420 and 1150–1180 cm^{-1} [48,49]. As weak spectral features appeared at these wavenumbers in the FTIR spectra of the Au samples, we cannot exclude the occurrence of this dissociation process.

As in the decomposition of methanol [27], the catalytic performance of the Au nanoparticles depended on the nature of the support. In the case of Au/Al_2O_3, the dehydration property of Al_2O_3 was so dominant that the effect of Au could not be expressed. As a result, hydrogen was not produced. On all the other Au samples, the main process was the dehydrogenation of ethanol (Eq. (2)). This occurred at the highest rate on Au/CeO_2, where more than 30% of the hydrogen content of the ethanol decomposed was converted into gaseous hydrogen (Fig. 4). The slight formation of methane and carbon monoxide, however, indicated that C–C bond cleavage also took place. As this was observed to only a limited extent, it is not surprising that the addition of water to the ethanol hardly influenced the product distribution, and particularly the formation of hydrogen.

In situ IR spectroscopic measurements on Au/CeO_2 at 573–773 K (Fig. 6) revealed the presence of adsorbed species which were already formed during the annealing of the adsorbed ethanol (Fig. 3): undissociated ethanol (1252 and 1383 cm^{-1}), ethoxy radical (2964, 2867, 1100 and 1054 cm^{-1}), acetate (1621, 1547 and 1427–1445 cm^{-1}) and crotonaldehyde (1620 and 1594 cm^{-1}). We additionally detected the formation of carbon monoxide (1900–1910 cm^{-1}), carbon dioxide (2361 and 2333 cm^{-1}) and acetaldehyde (1700–1686 cm^{-1}), which is in harmony with the product distribution of the catalytic reaction at high temperatures.

An important feature in the explanation of the high activity of Au/CeO_2 is the fact that pure CeO_2 also catalyses the decomposition of ethanol, though only at 673–773 K. At 623 K, the conversion of ethanol on CeO_2 was only ~15%, whereas on 1% Au/CeO_2 it was 80%. All these findings clearly suggest a cooperative effect between the Au nanoparticles and the CeO_2 support. We may assume that Au/CeO_2 contains very reactive sites, one possibility being the interface between the Au and the partially reduced CeO_x, where an electronic interaction occurs between the Au and the n-type CeO_2 semiconductor, similar to that discovered first between Ni and n-type TiO_2 [50,51]. With regard to the ready formation of the ethoxy radical in the adsorption and reaction of ethanol on the solids studied (Table 1, Figs. 2 and 6), it seems very likely that the rate-determining step in ethanol decomposition is the rupture of one of the ethoxy C–H bonds:

$$C_2H_5O_{(a)} = C_2H_4O_{(a)} + H_{(a)} \quad (5)$$

The characteristic catalytic behaviour of Au/CeO_2 was also manifested in the product distribution. The decomposition of acetaldehyde, the primary product in the dehydrogenation reaction, to methane and carbon monoxide:

$$CH_3CHO_{(a)} = CH_4 + CO \quad (6)$$

proceeded to only a very limited extent. Instead, it was converted into various hydrocarbons and oligomerized into 2-pentanone and 3-penten-2-one. These latter compounds were detected in small quantities on pure CeO_2 too, but their amounts were markedly enhanced in response to increasing Au loading. Their formation has not been reported previously on ceria-supported transition metals [29,36,37,45–47,52,53], which effectively catalysed the decomposition of acetaldehyde according to Eq. (6). It is to be emphasized that these compounds were found only on ceria-based catalysts. Exploratory studies on the reaction of acetaldehyde on Au/CeO_2 proved that 2-pentanone and 3-penten-2-one are formed on this sample above 623 K. Further studies are clearly required to evaluate the role of Au/CeO_2 in the reaction of acetaldehyde.

As the dominant reaction pathway is the dehydrogenation of ethanol, C–C bond rupture resulting in the formation of carbon monoxide and methane occurs to only a limited extent, it is not surprising that the addition of water to the ethanol exerted only a very slight effect on the product distribution.

5. Conclusions

(i) XPS characterization of supported Au samples reduced at 673 K revealed the simultaneous presence of Au^{3+}, Au^{1+} and Au^0 on the surfaces.
(ii) FTIR and TPD studies on pure and Au-containing SiO_2 demonstrated that the ethoxy radical is formed on the Au particles at 300 K and decomposes into various compounds above 400 K.
(iii) Au nanoparticles deposited on various supports proved to be an active catalyst for the dehydrogenation of ethanol. The formation of hydrogen and the product distribution depended sensitively on the nature of the support. The highest rate of hydrogen evolution was observed on Au/CeO_2. No deactivation of the Au/CeO_2 catalyst was experienced in ~8 h at 623 K.
(iv) The acetaldehyde formed on Au/CeO_2 in the dehydrogenation of ethanol is converted into various products, including C_5 oxo compounds.

Acknowledgements

This work was supported by OTKA under contract number NI 69327. The authors express their thank to Mr. P. Németh for TEM measurements, and to Dr. M. Dömök for GM-MS measurements.

References

[1] G. Sandstede, T.N. Veziroglu, C. Derive, J. Pottier (Eds.), Proceedings of the Ninth World Hydrogen Energy Conference, Paris, France, 1972, p. 1745.
[2] A. Haryanto, S. Fernando, N. Murali, S. Adhikari, Energy Fuels 19 (2005) 2098.
[3] L.F. Brown, Int. J. Hydrogen Energy 26 (2001) 381.
[4] N. Muradov, Catal. Commun. 2 (2001) 89.
[5] T.V. Choudhary, E. Aksoylu, D.W. Goodman, Catal. Rev. Sci. Eng. 45 (2003) 151.
[6] R.A. van Santen, A. de Koster, T. Koerts, Catal. Lett. 7 (1990) 1.
[7] F. Solymosi, Gy. Kutsán, A. Erdőhelyi, Catal. Lett. 11 (1991) 149.
[8] F. Solymosi, A. Erdőhelyi, J. Cserényi, Catal. Lett. 16 (1992) 399.
[9] M. Belgued, H. Amariglio, P. Pareja, A. Amariglio, J. Sain-Just, Catal. Today 13 (1992) 437.
[10] T. Koerts, M.J.A.G. Deelen, R.A. van Santen, J. Catal. 138 (1992) 101.
[11] F. Solymosi, A. Erdőhelyi, J. Cserényi, J. Catal. 147 (1994) 272.
[12] F. Solymosi, J. Cserényi, Catal. Today 21 (1994) 561.
[13] A. Erdőhelyi, J. Raskó, T. Kecskés, M. Tóth, M. Dömök, K. Baán, Catal. Today 116 (2006) 367.
[14] J. Raskó, M. Dömök, K. Baán, A. Erdőhelyi, Appl. Catal. A: Gen. 299 (2006) 202.
[15] A.C. Basagiannis, P. Panagiotopoulou, X.E. Verykos, Top. Catal. 51 (2008) 2.
[16] R. Barthos, A. Széchenyi, F. Solymosi, Catal. Lett. 120 (2008) 161.
[17] R. Barthos, A. Széchenyi, Á. Koós, F. Solymosi, Appl. Catal. A: Gen. 327 (2007) 95.
[18] R. Barthos, F. Solymosi, J. Catal. 249 (2007) 289;
Á. Koós, R. Barthos, F. Solymosi, J. Phys. Chem. C 112 (2008) 2607.
[19] F. Solymosi, R. Barthos, A. Kecskeméti, Appl. Catal. A: Gen. 350 (2008) 30.
[20] M. Haruta, T. Kobayashi, H. Sano, N. Yamada, Chem. Lett. (1987) 405.
[21] A.S.K. Hashmi, G.J. Hutchings, Angew. Chem. Int. Ed. 45 (2006) 7896.
[22] J.G. Hardy, M.W. Roberts, Chem. Commun. (1971) 494;
M.W. Roberts, T.I. Stewart, in: P. Hepple (Ed.), Proceedings of Chemisorption and Catalysis, Institute of Petroleum, 1970.
[23] M. Haruta, A. Ueda, S. Tsubota, R.M. Torres Sanchez, Catal. Today 29 (1996) 443.
[24] A. Nuhu, J. Soares, M. Gonzalez-Herrera, A. Watts, G. Hussein, M. Bowker, Top. Catal. 44 (2007) 293.
[25] F. Boccuzzi, A. Chiorino, M. Manzoli, J. Power Sources 118 (2003) 304.
[26] M. Manzoli, A. Chiorino, F. Boccuzzi, Appl. Catal. B: Environ. 57 (2005) 201.
[27] A. Gazsi, T. Bánsági, F. Solymosi, Catal. Lett. 131 (2009) 33.
[28] I. Mitov, D. Klissurski, C. Minchev, C. R. De L. Acad. Bulg. Des. Sci. 61 (2008) 1003.
[29] P.-Y. Sheng, G.A. Bowmaker, H. Idriss, Appl. Catal. A: Gen. 261 (2004) 171.
[30] Y. Guan, E.J.M. Hensen, Appl. Catal. A: Gen. 361 (2009) 49.
[31] E.D. Park, J.S. Lee, J. Catal. 186 (1999) 1.
[32] A. Karpenko, R. Leppelt, V. Plzak, R.J. Behm, J. Catal. 252 (2007) 231.
[33] P. Burroughs, A. Hamnett, A.F. Orchard, G. Thornton, J. Chem. Soc., Dalton Trans. (1976) 1686.
[34] J.P. Holgado, R. Alvarez, G. Munuera, Appl. Surf. Sci. 161 (2000) 301.
[35] M. Skoda, M. Cabala, I. Matolínová, K.C. Prince, T. Skála, F. Sutara, K. Veltruská, V. Matolín, J. Chem. Phys. 130 (2009) 034703, and references therein.
[36] M.A. Natal-Santiago, J.A. Dumesic, J. Catal. 175 (1998) 252.
[37] A. Yee, S.J. Morrison, H. Idriss, Catal. Today 63 (2000) 327.
[38] A. Yee, S.J. Morrison, H. Idriss, J. Catal. 186 (1999) 279.
[39] A.P. Farkas, F. Solymosi, Surf. Sci. 602 (2008) 1475, and references therein.
[40] B.A. Sexton, Surf. Sci. 88 (1979) 299.
[41] Q. Dai, A.J. Gellman, Surf. Sci. 257 (1991) 103.
[42] J.L. Davis, M.A. Barteau, Surf. Sci. 235 (1990) 235.
[43] J. Gong, B. Mullins, J. Am. Chem. Soc. 130 (2008) 16458.
[44] S. Strbac, M.A. Ivic, Electrochim. Acta 54 (2009) 5408.
[45] H. Idriss, C. Diagne, J.P. Hindermann, A. Kiennemann, M.A. Barteau, J. Catal. 155 (1995) 219.
[46] P.-Y. Sheng, A. Yee, G.A. Bowmaker, H. Idriss, J. Catal. 208 (2002) 393.
[47] H. Madhavaram, H. Idriss, J. Catal. 224 (2004) 358.
[48] L. Bugyi, A. Oszkó, F. Solymosi, J. Catal. 159 (1996) 305.
[49] F. Solymosi, L. Bugyi, A. Oszkó, Langmuir 12 (1996) 4145.
[50] Z.G. Szabó, F. Solymosi, Actes Congr. Intern. Catalyse 2e Paris 1960 (1961) 1627.
[51] F. Solymosi, Catal. Rev. 1 (1968) 233.
[52] H. Song, U.S. Ozkan, J. Catal. 261 (2009) 66.
[53] H. Song, B. Tan, U.S. Ozkan, Catal. Lett. 132 (2009) 422.